Cracks in Thin Sheets: When Geometry Rules the Fracture Path

B. Audoly,[1] P. M. Reis,[2] and B. Roman[3]
[1]LMM, UMR 7607 CNRS/UPMC, 4 place Jussieu, case 162, 75252 Paris cedex 05, France
[2]Manchester Center for Nonlinear Dynamics, University of Manchester, M139PL United Kingdom
[3]PMMH, UMR 7636 CNRS/ESPCI, 10 rue Vauquelin 75231 cedex 5 Paris, France
(Received 17 October 2004; published 7 July 2005)

We study the propagation of brittle fractures coupled to large out-of-plane bending, as when a brittle elastic thin sheet is cut by a moving object. Taking into account the separation of the film's bending and stretching energies and using fracture theory we show that such cracks propagate according to a simple set of geometrical rules in the limit of small thickness. In particular, this provides some insight into the geometrical origin of the oscillatory fracture patterns reported in two recent experiments. Numerical integration of our geometrical rules accurately reproduces both the shape of the fracture pattern and the detailed time evolution of the propagation of the crack tip, for various geometries of the cutting object.

DOI: 10.1103/PhysRevLett.95.025502 PACS numbers: 62.20.Mk, 46.50.+a, 46.70.De

A fascinating problem in fracture theory concerns the prediction of the crack path and the associated instabilities: when a piece of material breaks, what determines the shape of the resulting pieces? Within the physics community, there has been a recent upsurge of interest in this question. For example, an oscillatory instability occurs in quasistatic propagation of cracks in thermally quenched strips of silicon and glass [1]. This simple experimental system has stimulated a number of theoretical and numerical studies [2]. Another instability has been observed when a biaxially strained thin rubber sheet is pierced and the crack propagates dynamically [3], the underlying mechanisms of which remains unclear.

In this Letter we perform an analysis of cracks propagating in thin elastic films. Previous studies of cracks in thin plates were concerned with the *ductile* limit [4], which is relevant in the engineering context of ship plating due to cutting, tearing or bending during collision or grounding [5]. Here, we focus on the opposite limit of *brittle* thin films. This limit is relevant for the analysis of a novel type of crack instability that has recently been reported by two independent studies [6,7].

In these experiments, a rigid object, the *cutting tool* is forced through a thin polymer film and tears through the material as it advances; see Fig. 1. The tool is oriented perpendicularly to the film. The film is clamped at its lateral boundaries which impose no initial tension and is driven parallel to its major length. The thin film is brittle, hence it undergoes negligible irreversible deformation besides fracture. For tools much wider than the film's thickness, the crack tip T follows a highly reproducible nonsinusoidal oscillatory path. Each single period of this path consists of two smooth curves separated by a kink, at which there is a sharp change in the direction of curvature. Propagation is primarily quasistatic, at a speed comparable to that of the cutting tool v, but is interrupted by periodic bursts of dynamic propagation immediately after each kink. By decreasing the size of the cutting tool down to widths comparable to the film thickness, the crack path eventually becomes straight, as reported in [6,7], but here we focus on the oscillatory behavior far above threshold. The film thickness h is therefore much smaller than any other dimension in the system. In this regime, the crack morphology is independent of v (as long as this remains much smaller than the speed of sound in the material), h (provided that $h \ll w$), and the film's width D. The only relevant length scale in the problem is the width of the cutting tool, w, with which both the pattern's amplitude, A, and wavelength, λ, have been found to scale linearly [6].

This simple experimental scaling law, together with the robustness of this instability, suggests that a simple underlying mechanism is at stake. Ghatak and Mahadevan [7] have proposed a simple picture of the experimental patterns, assuming that the crack tip moves along the tool's circumference at a constant velocity with alternating direction. However, this description only crudely mimics what is observed in the experiments [8] and it is not based

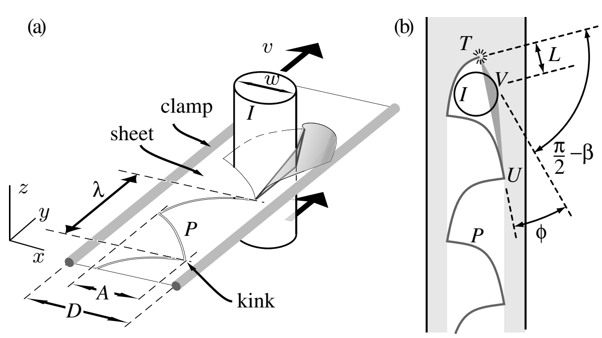

FIG. 1. (a) Schematic of an oscillatory path P, obtained when a cutting tool I, is driven at constant velocity v, through a thin polymer film clamped at two of its lateral boundaries [6]. λ and A are the wavelength and amplitude of the pattern, respectively. (b) Our 2D model divides the film into three regions: the *soft region* (white) where the presence of the tool I is accommodated by mere bending of the film, the *active region* (TVU) (dark gray) where the elastic energy is stored and the *outer region* (light gray).

on principles of mechanics even though the equations for thin plates are well known [9].

Here, we show that the classical equations for elastic plates and for crack propagation can be reduced to a simple set of *geometrical rules* which explain the experimentally observed crack behavior in the thin brittle films, mentioned above. Following a common approach in fracture theory, we first calculate the elastic energy of the system, taking into account the possible large out-of-plane deformations of the film induced by the cutting tool. Secondly, we apply Griffith's criterion for crack propagation and finally establish the direction of propagation of the crack tip.

Deformations of thin films satisfy a set of nonlinear partial differential equations, such as the Föppl–von Kármán equations [9], which makes the description of fracture of thin sheets a challenging endeavor. Fortunately, the following remarks make it unnecessary to resort to the full equations. In the limit of small film aspect ratio, $h/D \ll 1$, (typically $h/D \sim 10^{-3}$ in the experiments), the elastic energy of a film decouples into a bending term, associated with curvature, and a stretching term, associated with longitudinal extension [10]. In thin films ($h \ll D$), the bending energy is formally negligible in front of the stretching one. This suggests that the driving forces for crack propagation lie in in-plane stretching [11]: the bending energy can be neglected, this way allowing large out-of-plane deformations of the film. This affects the repartition of tensile stresses in a manner that we now investigate.

Consider a cylindrical cutting tool I, and a partial crack path P in the sheet. We call the *soft zone* the region shown in white in Fig. 1(b), which is mathematically defined as the convex hull [12] of the crack path. This soft zone has the particular mechanical property that, as long as the projection of the cutting tool onto the film plane remains fully contained within this zone, the sheet merely bends away, with negligible stretching, to accommodate its presence. The resulting elastic energy is pure bending and, as stated before, is insufficient to make the crack propagate.

In contrast, when the projection of the cutting tool moves beyond one of the boundaries of the soft zone, as in Fig. 1(a), the film is stretched and stores a substantial amount of elastic energy. In Fig. 1(a), the flap with large out-of-plane deformation is connected to the plane of the film along a sharp fold. It is important to note that this fold is pushed upon by the cutting tool and, as a result, is stretched. In the projection onto the film plane [see Fig. 1(b)] this stretching is apparent as the initially straight segment $[TU]$ becomes a broken line $[TVU]$. Any point initially located inside the region (TVU) will similarly undergo tensile in-plane stresses. Hence, a strain $\epsilon \approx \mathcal{L}(TVU)/\mathcal{L}(TU) - 1 \approx \phi^2/2$, develops in the film, where $\mathcal{L}(.)$ denotes the length of a broken line. The angle $\phi \ll \pi/2$ is defined by the boundary of the soft zone, $[TU]$, and the outmost edge of the cutting tool, V [see Fig. 1(b)]. The triangle $[TVU]$, shown in dark gray in Fig. 1(b), is the region of large tensile in-plane strain which we call the *active region*, denoted by $\mathcal{A}(P, I)$.

We claim that the tensile stresses concentrated in this active region are the driving force for crack propagation. The elastic energy of the film can be estimated as

$$\mathcal{E}(P, I) = Eh \iint_{\mathcal{A}(P,I)} dxdy\epsilon^2(x, y) \approx \frac{EhL^2\phi^5}{40}, \quad (1)$$

where the integration is done over the active region $\mathcal{A}(P, I)$, x and y are the coordinates along the plane of the film, L is the distance between the crack tip and the cutting tool, and E is the Young's modulus of the film. An order of magnitude estimation follows by noting that the tensile in-plane strain inside the active region, $\epsilon(x, y)$, is of order ϕ^2 and the prefactor $1/40$ can be obtained with a more detailed estimate of the stress distribution in this active region.

To address the propagation of the crack tip, we now apply Griffith's criterion [13] which is a balance between the elastic energy stored in the material and that dissipated near crack tip at the microscopic level (by atomic or molecular bonds breaking, by nucleation of defects, etc.). These dissipative processes can collectively be taken into account by introducing an overall effective toughness Γ, with dimensions of surface tension. Hence, any advance of the crack tip by $\delta\ell$ dissipates an energy $\Gamma h \delta\ell$. This toughness, Γ, is a function of the material considered and may also depend on the type of loading at the crack tip but, here, we make the simplifying assumption that Γ is constant throughout the cutting process.

By balancing [14] the release rate of elastic energy, $\delta\mathcal{E}/\delta\ell \approx (\partial\mathcal{E}/\partial\phi)\delta\phi/\delta\ell$, with the rate of energy dissipation per unit of new crack length, Γh, and by further noticing that $\delta\phi/\delta\ell$ is given by geometry as $1/L$, we obtain the following propagation criterion from the energy estimation in Eq. (1):

$$\delta\mathcal{E}/\delta\ell \geq \Gamma h \Rightarrow \phi \geq \alpha \quad \text{with } \alpha = [8\Gamma/(EL)]^{1/4}. \quad (2)$$

Here, α reflects the fracture properties of the material, while ϕ measures the penetration of the tool into the film. When this inequality is satisfied, there is enough energy available for the crack to propagate, otherwise it remains at rest. The weak dependence on L with a power $1/4$ makes it a good approximation to replace, in Eq. (2), the variable distance L by the constant cutting tool's width w, both being of the same order of magnitude. Therefore, in the numerical simulations, we take α as a fixed parameter.

The final point to address is the direction of propagation of the crack tip. The classical *principle of local symmetry* assumes that the direction that cancels any mode *II* loading (in-plane shear) is selected [15]. As discussed above, the driving force for propagation is associated with the stretching of the active zone along the segment $[TU]$. This implies that, near the crack tip, the stresses are essentially opening (mode *I*), in a direction parallel to the edge of the active zone, (TV). By the principle of local symmetry, the direction of crack propagation is expected to be approximately perpendicular to this direction: the angle β, defined in Fig. 1(b) as $\pi/2$ minus the angle between the edge $[TV]$ of the active region and the direction of propagation, must therefore be small and is taken to be a constant.

For simplicity, our fracture model has been presented when the cutting tool has a circular cross-section. For an arbitrary section, it can be implemented in the following sequence, which extends the previous construction: (i) compute the convex hull of the crack path, which yields the soft region; (ii) determine the union of the crack path with the cutting tool, and then its convex hull; (iii) calculate the set difference of this convex hull minus the soft region, yielding the active region; (iv) compute the angle ϕ; (v) if $\phi \geq \alpha$, propagate the crack along a direction given by β until ϕ decreases back below α. This algorithm predicts the evolution of the crack tip's position using a *2D geometrical construction* and elasticity is reflected by the two model parameters: α and β.

We have performed simulations of this geometrical algorithm and found that spontaneous oscillations of the crack are obtained for generic values of the parameters α and β: the tool alternatively pushes on either lip of the crack, every change of lip producing a kink. Typical frames from the numerical simulations are shown in Fig. 2. Our model is able to portray the main features of the cracks found experimentally [6,7] and reproduces the detailed time evolution of the crack tip's position. All the material properties of the film are reflected in α and β which, indeed, makes the width of the cutting tool the only relevant length scale. This explains why, within the regime we are considering of $w \gg h$, both the amplitude and wavelength of the crack pattern scale linearly with w and are independent of D, v, and h.

We proceed by comparing the oscillatory cracks obtained from our geometrical model to the experiments reported in [6]. In this comparison, a single type of bioriented polypropylene film with $h = 50$ μm is used in the experiments (the influence of the film properties has already been documented elsewhere [6,7]). The parameters α and β were therefore set to fixed values, determined once for all by performing a single least squares fit between a series of numerical and an experimental paths corresponding to a variety of indenter shapes (including circular, square, and rectangular cross-sections). This yielded the values $\alpha = 0.20$, $\beta = 0.03$ which were then used throughout, without further adjustment. Note that the value $\alpha = 0.20$ is consistent with an estimate of Eq. (2), for length scales of order 10^{-2} m, using the experimentally measured values of $\Gamma \sim 1$ kJ/m^2 and $E \sim 1$ GPa for the particular film we are considering.

In Fig. 3 we present the numerical results for a cylindrical tool (solid lines) as a typical example, which we compare against experiments [6] with $w = 20.4$ mm (dashed lines). Excellent agreement is found between the two. In particular, both the kinks and the subsequent bursts of dynamic propagation arise from the simple set of rules (i)–(v). These are, therefore, intrinsic features of the tearing process, which can be understood as follows. Because of the geometry of the system, as the tool advances there are two components to the active zone: to the left, S, and to the right, S', of the cutting tool (see Fig. 2). At almost all times, only one of these two zones defines a nonzero angle ϕ at the crack tip [see Fig. 2(a)] and thus contributes to crack advance. However, when this nonzero angle switches from the left to the right of the crack tip, there is a short period of time (whose duration, relative to a period, is of the order of the small number α) where both angles are nonzero: in the frame of Fig. 2(b), for instance, ϕ has been equal to the critical value α since the previous kink, while ϕ' is rapidly increasing as the tool penetrates into the right hand side rim of the film. The crack bifurcates exactly at the frame of Fig. 2(b), when both angles become equal: $\phi = \phi' = \alpha$. Immediately after this kink, the propagation criterion is overshoot ($\phi' > \alpha$) and a finite advance of the crack is needed for the equality in Eq. (2) to be satisfied

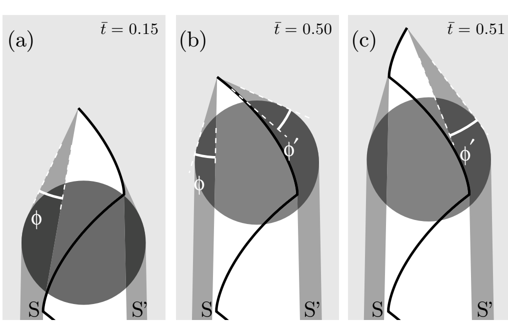

FIG. 2. Typical frames from numerical simulations for various dimensionless times $\bar{t} = vt/\lambda$: (a) during quasistatic propagation; (b) just before and (c) just after a kink followed by a burst of dynamic propagation. The soft, stretched, and outer regions are shown in white, dark gray, and light gray, respectively. The circle in gray represents the cutting tool. In frame (b), the active region has two components S and S' which define two nonzero angles ϕ and ϕ' at the tip.

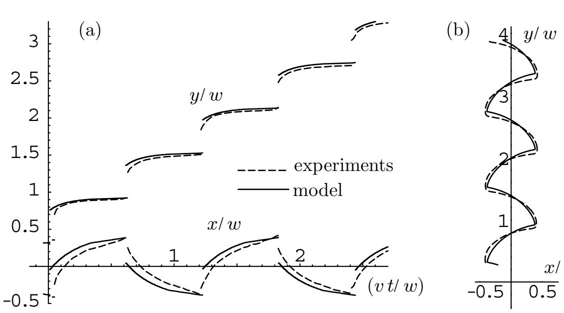

FIG. 3. Comparison of crack tip motion from the model and the experiments for a cylindrical cutting tool ($w = 20.4$ mm, $h = 50$ μm, $v = 1.2$ mm $\cdot$ s^{-1}). The model's parameters were $\alpha = 0.20$ and $\beta = 0.03$. (a) Time series for the crack tip coordinates $x(t)/w$ and $y(t)/w$ as a function of nondimensionalized tool advance, vt/w. Note the periodic gaps in crack position, corresponding to dynamic propagation. (b) Final pattern in the film plane (x, y).

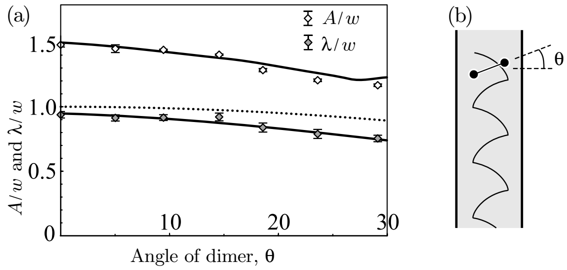

FIG. 4. (a) Comparison of experimental (data points) and numerical (solid curves) crack patterns, with a cutting tool made of a dimer (two parallel cylinders with diameter $d =$ 3.95 mm, with axes separated by $l = 12$ mm, overall width being $w = d + l$) tilted at variable angle θ, as in (b). Rescaled amplitude, A/w, and wavelength, λ/w are given as a function of tilt angle θ. Although this tool is considerably different from that of Fig. 3, no parameter was further adjusted. Both the experimental and numerical curves deviate significantly from the naive prediction, shown in dotted line, that the pattern amplitude is given by the dimer's frontal width, $d + l\cos\theta$.

($\phi' = \alpha$), see Fig. 2(c). This dynamic propagation event can be interpreted as the sudden release of the elastic energy stored into region S' between the frames in Figs. 2(a) and 2(b).

As our theory makes no particular assumption on the tool geometry, it can be applied just as well to noncylindrical geometries. We have indeed tested it in a considerably different geometry whereby the cutting tool consisted of a dimer with *two* parallel cylinders of diameters $d =$ 3.95 mm, rigidly separated by $l = 12$ mm. This dimer could be tilted at a variable angle θ with respect to the transverse direction of the film, as shown in Fig. 4(b). In Fig. 4(a), the experimental and numerical wavelengths and amplitude of the patterns obtained for various values of the tilt angle θ are shown to be in good agreement. We have used the same fixed values of $\alpha = 0.20$ and $\beta = 0.03$ as before. Another interesting prediction of the model, which we have confirmed experimentally, is that this dimer configuration yields a crack path rigorously identical to that obtained with a flat blade with the same cross-section dimensions, $(d + l) \times d$, since both of these cutting tools have the same convex hull.

Starting from the principles of elasticity, we have shown that the dynamics of cracks in thin brittle sheets is ruled by a simple 2D geometrical construction, based on the interplay between crack propagation and large out-of-plane deformations in the film. The direction of loading at the crack tip depends on the relative position of the crack tip and the cutting tool and thus is time dependent, while the intensity of loading depends on the full crack path (geometry of the soft region). This coupling leads to complex crack patterns, such as those recently reported in experiments where a rigid object cuts through the film. The detailed shape of these experimental fracture paths and the motion of the crack tip are accurately reproduced by simulations of our model. Our construction provides a general framework which can be applied, in particular, to tools with arbitrary cross-sections. Geometry, in general, is known to play an important role in the theory of elastic rods, plates, and shells. In the tearing of thin films, geometrical considerations acquire an unprecedented level of importance: to our knowledge, this is the first example where a complex crack motion is entirely ruled by geometry.

[1] A. Yuse and M. Sano, Nature (London) **362**, 329 (1993); O. Ronsin, F. Heslot, and B. Perrin, Phys. Rev. Lett. **75**, 2352 (1995); R. Deegan *et al.*, Phys. Rev. E **67**, 66209 (2003).
[2] B. Yang and K. Ravi-Chandar, J. Mech. Phys. Solids **49**, 91 (2001); M. Adda-Bedia and Y. Pomeau, Phys. Rev. E **52**, 4105 (1995); H. Henry and H. Levine, Phys. Rev. Lett. **93**, 105504 (2004); M. Adda-Bedia and M. Ben Amar, Phys. Rev. Lett. **76**, 1497 (1996).
[3] R. Deegan, P. Petersan, M. Marder, and H. Swinney, Phys. Rev. Lett. **88**, 014304 (2002).
[4] E. Sharon and B. Roman, Nature (London) **419**, 579 (2002); B. Audoly and A. Boudaoud, Phys. Rev. Lett. **91**, 086105 (2003).
[5] H. Vaughan, Nav. Archit. **97**, 97 (1978); T. Wierzbicky and P. Thomas, Int. J. Mech. Sci. **35**, 209 (1993).
[6] B. Roman *et al.*, C. R. Mécanique **331**, 811 (2003); See EPAPS Document No. PRLTAO-95-026527 for movies of the experiments and simulations. Please choose file "index.html". A direct link to this document may be found in the online article's HTML reference section. The document may also be reached via the EPAPS homepage (http://www.aip.org/pubservs/epaps.html) or from ftp.aip.org in the directory /epaps/. See the EPAPS homepage for more information.
[7] A. Ghatak and L. Mahadevan, Phys. Rev. Lett. **91**, 215507 (2003).
[8] B. Audoly, B. Roman, and P. M. Reis, Phys. Rev. Lett. **94**, 129601 (2005).
[9] L. D. Landau and E. M. Lifschitz, *Theory of Elasticity* (Pergamon, New York, 1959).
[10] A. Pogorelov, *Bending of Surfaces and Stability of Shells, Translation of Mathematical Monographs* (American Mathematical Society, Providence, 1988).
[11] That bending energy is too small to influence crack propagation can be confirmed by sharply creasing a plastic film between two fingers. This leads to permanent marks (hence much higher curvatures than in our experiments) but does not suffice to break the film.
[12] A convex hull is the smallest convex set that contains a given subset, here the crack path P.
[13] A. A. Griffith, Phil. Trans. R. Soc. A **221**, 163 (1921).
[14] In Griffith's criterion, the increment of crack length is *virtual* and occurs while the tool is stationary. This is analogous to writing a condition of stationary energy, $d\mathcal{E} = 0$, for *virtual* changes of state dx of a system at equilibrium.
[15] R. V. Goldstein and R. Salganik, Int. J. Fract. **10**, 507 (1974).